THE PENNSYLVANIA STATE UNIVERSITY
SCHREYER HONORS COLLEGE

DEPARTMENT OF AEROSPACE ENGINEERING

INVESTIGATION OF THE USE OF BEVELED NOZZLES FOR JET NOISE REDUCTION

MAUREEN SENFT
SPRING 2011

A thesis
submitted in partial fulfillment
of the requirements
for a baccalaureate degree
in Aerospace Engineering
with honors in Aerospace Engineering

Reviewed and approved* by the following:

Dennis K. McLaughlin
Professor of Aerospace Engineering
Thesis Supervisor

Robert G. Melton
Professor of Aerospace Engineering
Honors Adviser

George A. Lesieutre
Professor and Head, Department of Aerospace Engineering

* Signatures are on file in the Schreyer Honors College.

ABSTRACT

In recent years increasing population density near airports and military bases and the development of more powerful engines for military aircraft has prompted the serious consideration of noise reduction techniques for the aircraft. This paper reports on aeroacoustic experiments with laboratory size models of the engine exhaust nozzles. Specifically the study explores the effect on high-speed jet noise of beveled converging-diverging (CD) nozzles whose exit planes are oblique to the normal direction of the exit. The jets of small-scale nozzles with bevel angles of 24 and 35 degrees are compared to a baseline nozzle, each with a design Mach number of 1.65 and an area ratio of 1.295. Techniques such as schlieren and shadowgraph are used to visualize density gradients within the flow. With these flow visualization techniques the deflection of the plume in the case of the beveled nozzles is shown to be much smaller than the deflection found with supersonic jets exhausting from beveled purely converging nozzles. The acoustic data gathered presents a promising situation, with a noise reduction of approximately 3dB in the direction of the peak polar angle in the quadrant aligned with the long lip of the beveled nozzle.

TABLE OF CONTENTS

LIST OF FIGURES

LIST OF TABLES

NOMENCLATURE

a_o	speed of sound
A_x	cross-sectional area of the nozzle at location x
A*	cross-sectional area of the nozzle at the throat
BBSAN	broadband shock associated noise
D_x	diameter of the nozzle at location x
D*	diameter of the nozzle at the throat
f_c	characteristic frequency
$\mathring{m}$	mass flow rate
M_d	design Mach number
Mlocal	local Mach number
M_j	jet mach number
NPR	nozzle pressure ratio
P_x	pressure at location x
P_o	stagnation pressure
T_x	temperature at location x
T_o	stagnation temperature
TTR	total temperature ratio
v_x	speed of the jet flow at location x
X_{st}	x station (location) in the direction of flow
% Δ Thrust	change in percent thrust from the thrust at the design mach number

ACKNOWLEDGEMENTS

The author would like to express gratitude to Candidate for Masters student Russell Powers for the beveled nozzle design. Thanks is also due to Russell Powers and post-doc fellow of the Aerospace Department Ching-Wen Kuo for their assistance in laboratory experiments. I am grateful for the advice and direction given by Professor of Aerospace Engineering Dennis McLaughlin.

Chapter 1

Introduction

Motivation

Recently an emphasis has been put on the reduction of jet noise, especially for military aircraft. Of particular concern in the military community is the effect that high-speed jet noise has on jet crews, as well as civilian communities located in close proximity to military bases. Typically jet powered aircraft are run at off-design conditions during take-off and landing, and so shock-associated noise is a concern as well as noise due to turbulent mixing.

There are three major types of jet noise that are of concern; noise due to turbulent mixing, broadband shock-associated noise, and screech tones under certain conditions. Mixing noise is due to instability waves in the shear layer, whereas broadband shock-associated noise and screech tones are caused when the instability waves intersect the shock cell structure in the potential core.[1]

Methods of High Speed Jet Noise Reduction

Many methods of noise reduction for aircraft have been proposed, including the use of chevrons, axisymmetric nozzles, and variable geometry nozzles. Some of these methods achieve noise reduction through aggressive mixing in the shear layer and by decreasing the length of the potential core. Another concept is to reduce noise in certain azimuthal angles. This is the case with axisymmetric nozzles. This study will focus on the effectiveness of using a beveled nozzle to reduce high-speed jet noise by reducing noise levels in the peak radiation sector.

The idea behind using beveled nozzles is to orient the long lip on the underside of the engine. This long lip side tends to act somewhat like a shield to noise radiating in the downward direction. It is also expected, however, that the noise radiated in the quadrant of the short lip is likely to be higher than in the direction of the long lip. In an aircraft operation this is of little consequence because the community is below the aircraft in standard flight, and higher noise levels above the aircraft have no undesirable consequences. Vishwanathan[2] has previously shown that there is significant noise reduction below the long lip of the nozzle. Additionally, it was found that the level of noise reduction increased as the jet velocity also increased.

Studies on the effect of bevels in purely converging nozzles have found that the noise reduction is largely due to deflection of the jet plume. In contrast to this, studies completed with beveled converging-diverging nozzles show that the noise reduction due to the use of beveled nozzles is not largely due to the deflection of the jet plume. Viswanathan[2] was the first to study the effects of bevels on converging-diverging supersonic nozzles in great detail.

Small Scale Model

The nozzle used in this study replicates the variable exhaust nozzle on the F/A-18 Hornet aircraft. The variable exhaust nozzle on the aircraft has a number of flat panels in both the convergent and divergent sections of the nozzle. Actuation of these panels enables active control of the area ratio of the nozzle. The small-scale models used in this study are 1/35 of the full-scale nozzle. In the past, results obtained from experiments involving small-scale models have compared favorably to medium scale tests performed at NASA Glenn Research Center.[3,4]

Chapter 2

Experimental Facilities and Procedures

Facility Overview

The experiments in beveled nozzle jet noise presented in this thesis were conducted in The Pennsylvania State University Jet Noise Facility. A schematic of the jet noise facility is presented in Figure 2-1. All experiments were conducted in the anechoic chamber. A thermometer, barometer, and hygrometer are installed on the wall of the anechoic chamber, from which temperature, pressure, and humidity are monitored on a regular basis during experiments. Fiberglass wedges cover all walls and other surfaces downstream of the jet to ensure that experiments are run in essentially free field conditions, in other words that sound energy travels away from the nozzle and is not reflected back. A mixture of helium and air is used to approximate the density characteristics of a heated jet. This technique has been used for a number of years and has closely matched results obtained when using traditional heated jets.[5]

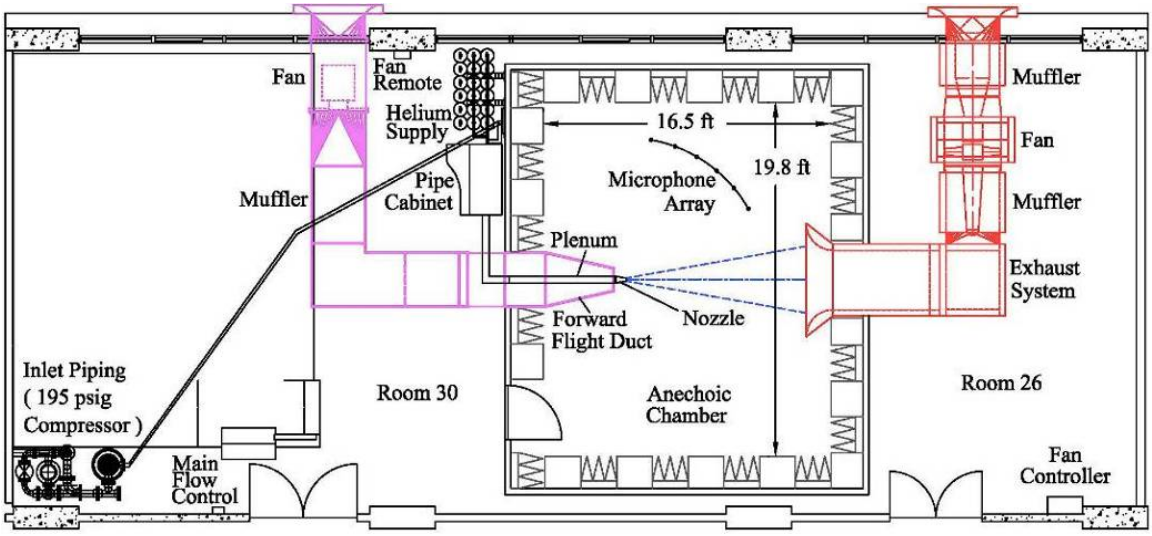

Figure 2-1. Schematic of the Pennsylvania State University Jet Noise Facility.

Experimental Setup

Acoustic measurements were obtained by using six 1/8 in. microphones oriented 10° away from each other in a microphone array. A picture showing the plenum and microphone array is shown in Figure 2-2, while Figure 2-3 shows the convention used for assignment of polar angles. During acoustic measurements the array was set to two different orientations so that measurements were obtained at angles of 20-70° and 80-150° at each jet condition. LabVIEW was used for acquisition of acoustic data, as shown in Figure 2-4. After the raw data was obtained Matlab was used to process the data and produce visuals of the acoustic spectra.

Figure 2-2. Photograph of the Plenum and Microphone Array

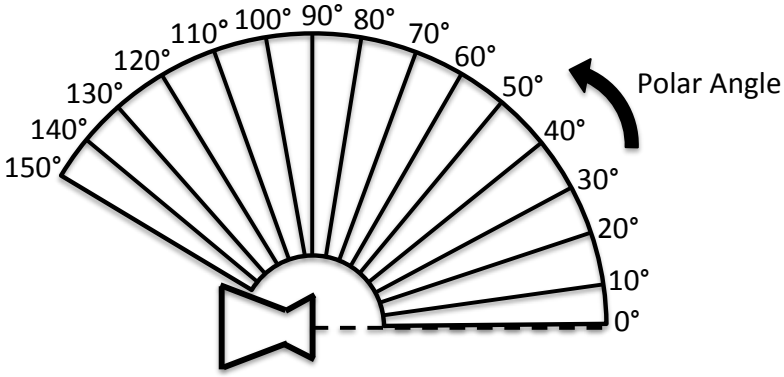

Figure 2-3. Polar Angle Convention.

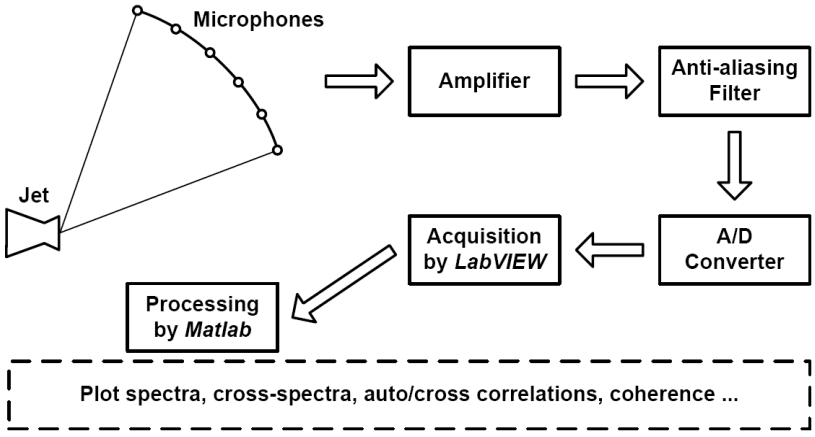

Figure 2-4. Overview of the Data Acquisition Process.

Flow Visualization Techniques

Two different methods were used to analyze the character of the flow. Shadowgraph was the first method used. It is a method by which disturbances that occur in a flow at high speeds can be visualized. Light which passes through the flow is refracted by density gradients, which show up as light and dark areas on the image. The experimental setup used for obtaining shadowgraph imagery can be seen in Figure 2-5. The methodology is very similar to schlieren flow visualization but does not use a knife edge. Settles[6] is an excellent reference for those who desire a more in depth understanding of shadowgraph and schlieren techniques. Both systems use a camera, and in our case the camera captured images at a rate of 60 images per second.

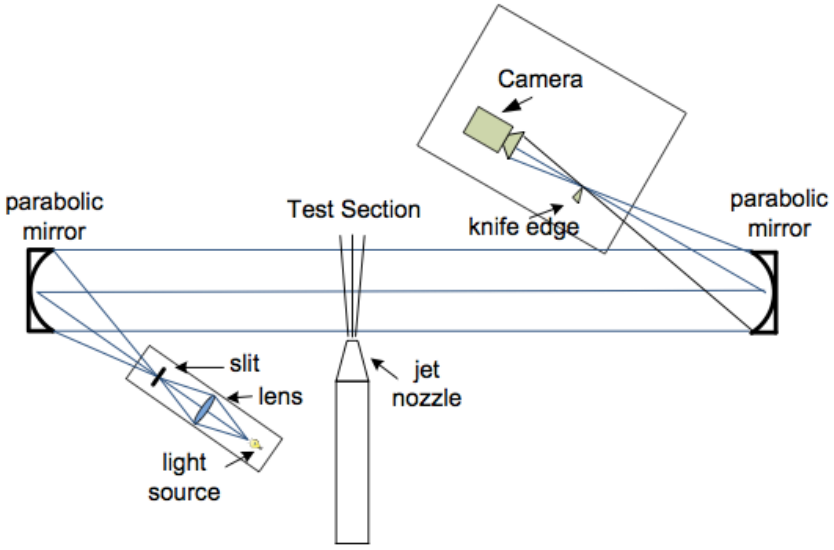

Figure 2-5. Shadowgraph and Schlieren Experimental Setup.

Nozzle Design

Three nozzles were used in these experiments. Bevel angles of 24° and 35° were chosen to compare to a round baseline nozzle (bevel angle 0°) with $M_d = 1.65$ and an area ratio of 1.295. Bevel angles of 24° and 35° were chosen because those angles have been previously studied in the area of noise reduction due to the use of beveled nozzles.[2] The dimensions of the baseline nozzle can be seen in Figure 2-6. The three nozzles were manufactured by rapid-prototyping using ABS injection. There are many methods which can be used to create a beveled nozzle from a round baseline nozzle. The method chosen in this study was decided upon because it results in a projected area ratio, or exit area which is perpendicular to the flow, which is approximately the same as the round baseline nozzle used. The method used to create the bevel is as follows. The middle of the rotation plane was set at the center of the nozzle exit plane. The rotation plane was then oriented to 24° and 35° from the baseline nozzle exit plane to create the 24° and 35° beveled nozzles, respectively. This process resulted in one lip of the nozzle being longer than the other. A

schematic of the rotation can be seen in Figure 2-7.

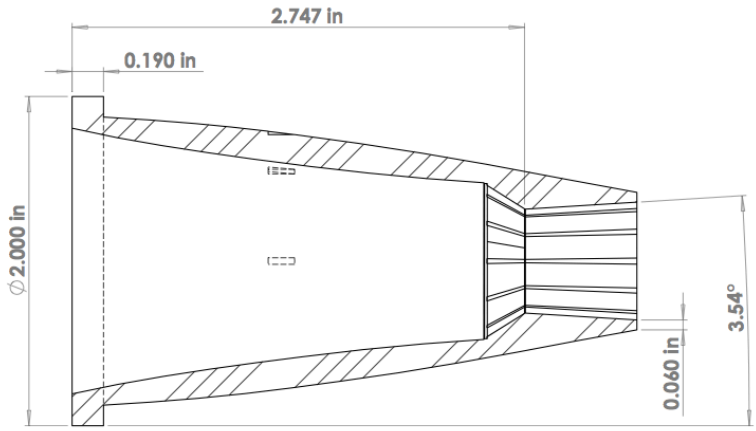

Figure 2-6. Baseline Nozzle Dimensions

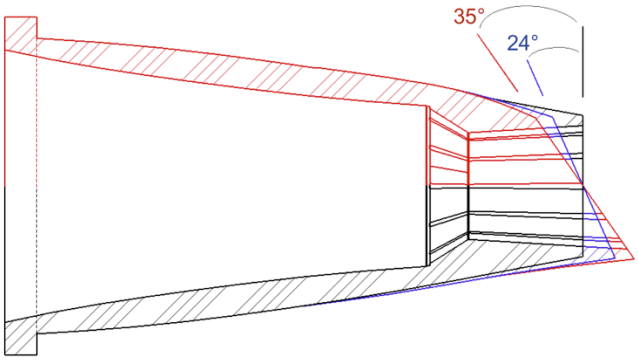

Figure 2-7. Bevel Design Methodology for the 24° and 35° Nozzles

Chapter 3

Experimental Results

Preliminary Calculations

Calculations were performed to obtain an estimate of the thrust and pressure characteristics of the flow at various x stations through the nozzle. The throat was designated as the origin, with the positive axis extending in the direction of the flow. Calculations were performed at different Nozzle Pressure Ratios (NPR). An abbreviated sample calculation is shown in Table 3-1 at NPR = 4. A row is manually entered at the point where the local Mach number is equal to the design Mach number for that NPR. Rows were also manually entered at area ratios of 1.16, 1.295, and 1.45, which correspond to the area ratio at the short lip, midpoint, and long lip, respectively. Values at the midpoint can be correlated to the baseline nozzle.

The equation used to calculate thrust is shown in Equation (1). The equation is composed of two different terms; one due to momentum, $\dot{m}*v_e$, and the other due to pressure, $(p_e-p_a)*A_e$. $\dot{m}$ represents the mass flow rate, while the pressure at location x and at ambient are represented by p_x and p_a, respectively. From these terms, thrust is calculated and then is nondimensionalized by dividing by (Po)A*, as seen in Table 3-1.

$$\text{Thrust} = \dot{m}*v_x + (p_x-p_a)*A_x \quad (1)$$

In Table 3-1 % Δ Thrust, or percent change in thrust, is determined by comparing the thrust at an x station to the thrust at the design Mach number for NPR = 4. As expected, when

thrust at the short lip, midpoint, and long lip is compared to thrust at the M_d there is a reduction. It is also apparent from the thrust calculations that at the short lip there is slightly more thrust than for the baseline nozzle, and at the long lip there is slightly less thrust than for the baseline. It is also expected that at take-off a jet with a beveled nozzle will have slightly more thrust than when using a baseline nozzle, and at cruise it will have about a .5% loss.

Table 3-1. Thrust and Pressure Calculations in the Nozzle, NPR = 4

Xst D*	Dx D*	Ax A*	Mlocal	Px Po	To Tx	Vx ao	Thrust (N)	Thrust (N) (Po)A*	% Δ Thrust
0.00	1.00	1.00	1.00	0.53	1.20	0.91	83.31	1.01787	-1.76
0.11	1.02	1.04	1.23	0.40	1.30	1.08	83.89	1.02500	-1.07
0.22	1.04	1.08	1.33	0.35	1.35	1.14	84.35	1.03064	-0.53
0.33	1.06	1.12	1.41	0.31	1.40	1.19	84.54	1.03290	-0.31
0.44	1.08	1.16	1.48	0.28	1.44	1.23	84.71	1.03500	-0.11
Short Lip		1.16	1.48	0.28	1.44	1.23	84.72	1.03511	-0.10
0.55	1.10	1.20	1.54	0.26	1.47	1.27	84.76	1.03567	-0.04
Design M for NPR = 4			1.56	0.25	1.49	1.28	84.80	1.03611	0.00
0.66	1.12	1.24	1.59	0.24	1.51	1.30	84.78	1.03593	-0.02
0.77	1.13	1.29	1.64	0.22	1.54	1.32	84.71	1.03504	-0.10
Midpoint		1.30	1.65	0.22	1.55	1.33	84.68	1.03469	-0.14
0.88	1.15	1.33	1.69	0.20	1.57	1.35	84.59	1.03359	-0.24
0.99	1.17	1.38	1.74	0.19	1.61	1.37	84.39	1.03107	-0.49
1.10	1.19	1.42	1.78	0.18	1.64	1.39	84.10	1.02759	-0.82
Long Lip		1.45	1.81	0.17	1.66	1.41	83.96	1.02581	-0.99

Figure 3-1, Figure 3-2, and Figure 3-3 show the pressure distribution inside the nozzle at various x locations. The x location is nondimensionalized by dividing the diameter at that particular x location by the diameter at the throat. The pressure on the y-axis is also nondimensionalized by dividing the pressure at the x location by the stagnation pressure. During calculations it was assumed that when the jet exhausts to atmosphere the pressure at the exit plane is equal to atmospheric pressure. From these types of graphs it can be determined whether the jet is overexpanded, perfectly expanded, or underexpanded at each location.

As with Table 3-1, Figure 3-1, Figure 3-2, and Figure 3-3 are a sample of the graphs

generated, and were chosen at NPR = 4 for the 35° beveled nozzle. Each graph has a dotted line which points from the location on the graph which represents when the jet exhausts to atmosphere to the section of the nozzle where that occurs. Figure 3-1 shows the pressure distribution at the short lip, Figure 3-2 shows the pressure distribution at the long lip, and Figure 3-3 overlays the pressure distribution at the short lip, midpoint (baseline), and long lip. From Figure 3-3 it is clear that at three locations the flow is overexpanded because p_x is greater than p_o inside the nozzle, and then at the exit plane p_x jumps up to p_a, or atmospheric pressure. In the case of the short lip the flow is only very slightly overexpanded.

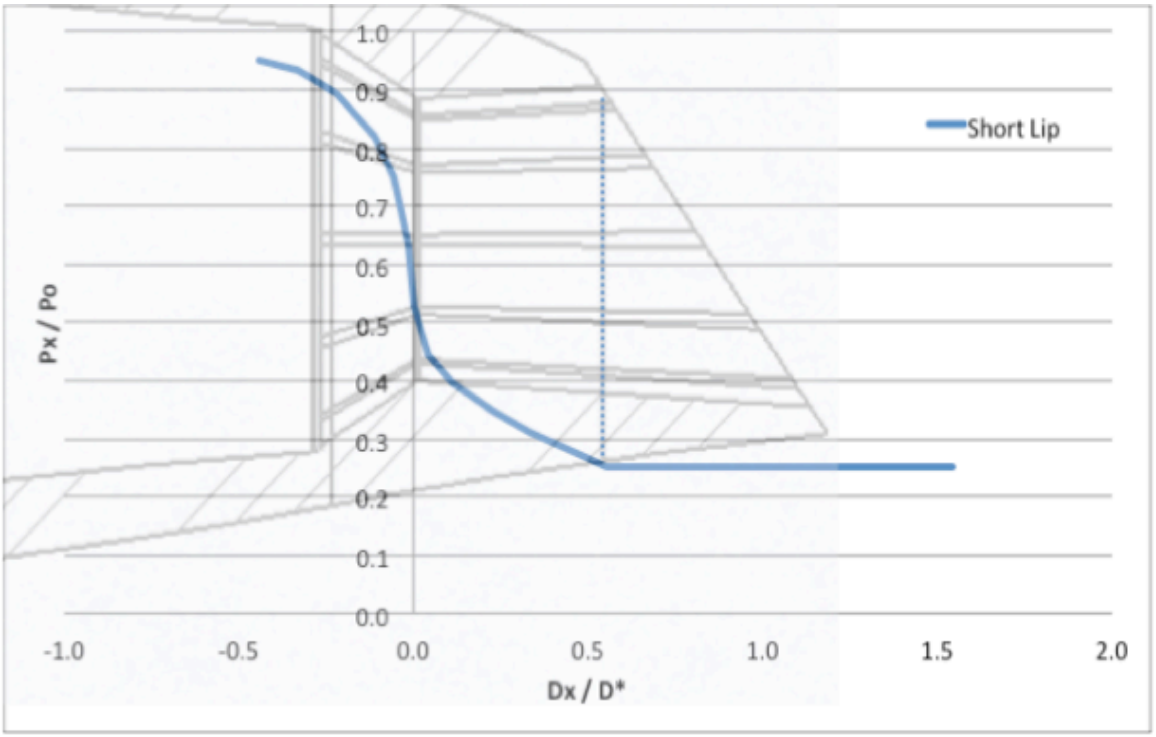

Figure 3-1. Pressure Distribution Inside the Nozzle at the Short Lip Side

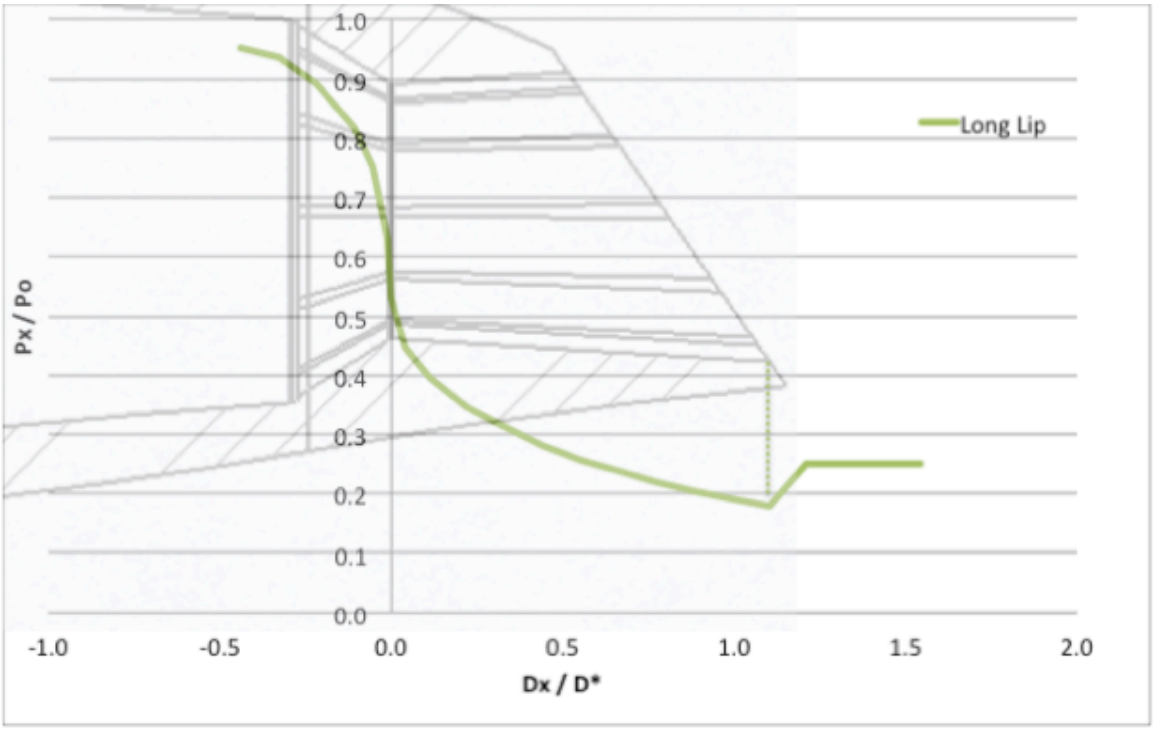

Figure 3-2. Pressure Distribution Inside the Nozzle at the Long Lip Side

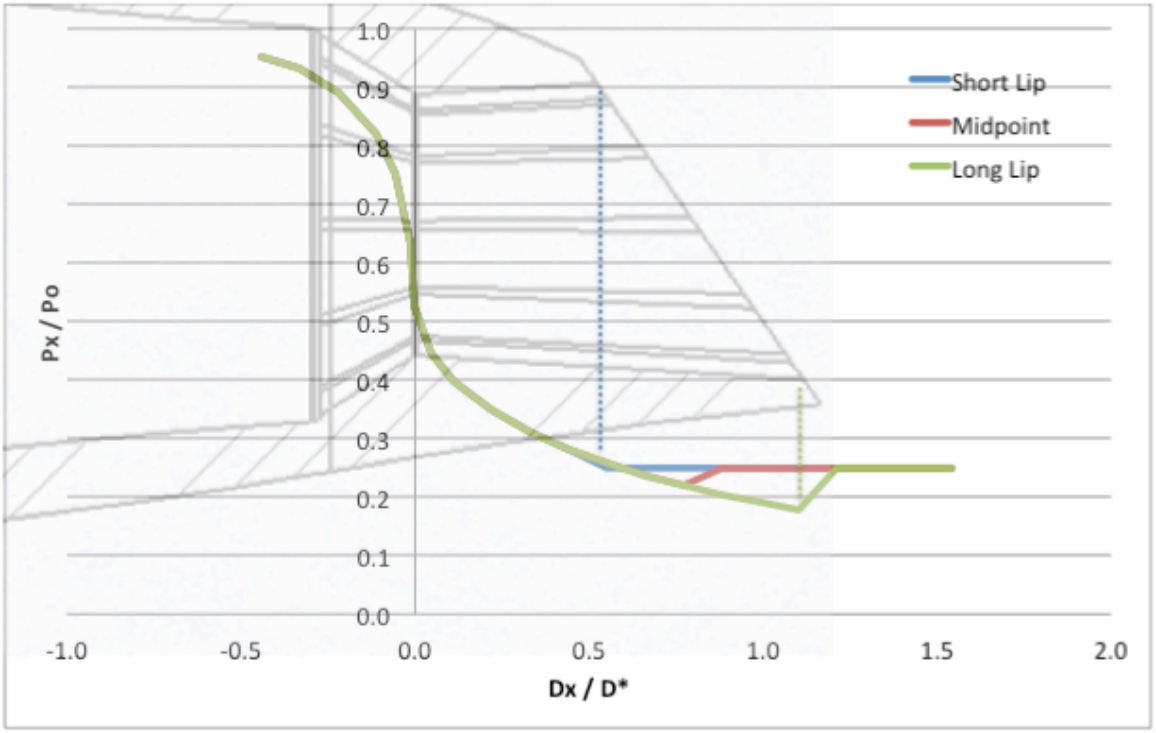

Figure 3-3. Overlay of the Pressure Distribution Inside the Nozzle at the Short Lip Side, Midpoint, and Long Lip Side

Flow Visualization

Two different methodologies, shadowgraph and schlieren imagery, were used to visualize the flow field. Nine different shadowgraph images are displayed in Figure 3-4 at M_j = 1.4, 1.6, and 1.9 for the baseline, 24° and 35° nozzles. In Figure 3-4, from the left to the right, the flow conditions are overexpanded, almost perfectly expanded, and underexpanded. Looking at the beveled nozzles, it can be seen that at overexpanded conditions the flow deflects towards the longer lip, with the angle of deflection increasing with the angle of the bevel. However, at underexpanded conditions the flow deflects towards the shorter lip. On average, for overexpanded conditions, the 24° beveled nozzle saw a 2.5° deflection of the flow, while the 35° beveled nozzle saw a 5° deflection. The level of deflection increased for the underexpanded case, with an

average of 3.2° for the 24° beveled nozzle and 6° for the 35° beveled nozzle.

Three other aspects of the flow field are of note. The first aspect is that in addition to the flow being deflected, Figure 3-4 shows that the shock cell structure also moves closer to the longer lip than the shorter lip for both overexpanded and underexpanded conditions. The second aspect is that the shock cell structure is elongated in the direction of the flow as the bevel angle increases. The third aspect is that shock cell strength increases with increasing bevel angle. Relative shock cell strength can be easily observed in shadowgraph imagery because stronger shock cells show up as darker lines in the images.

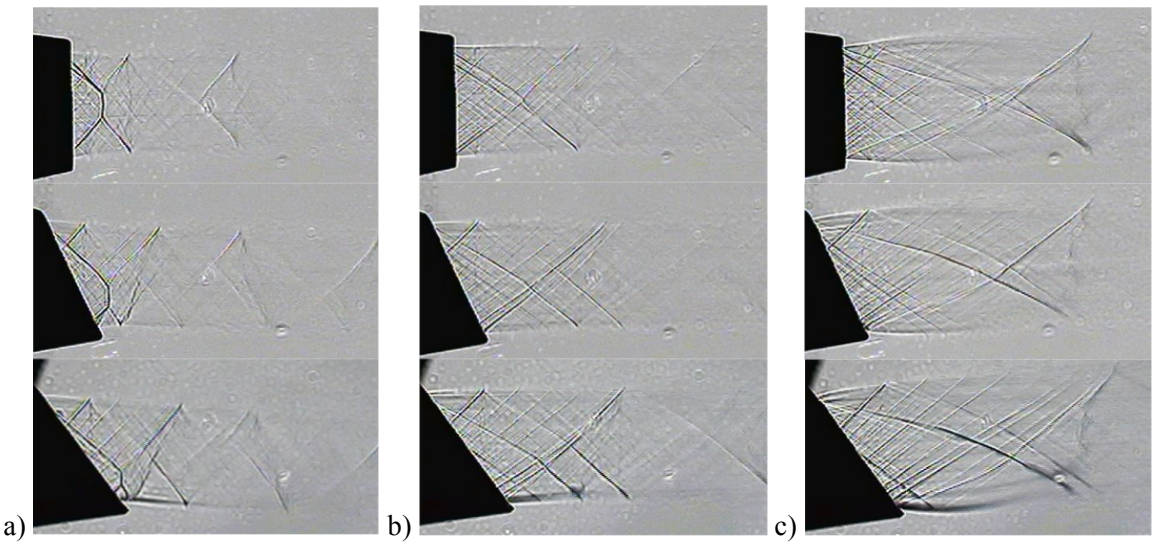

Figure 3-4. Shadowgraph Imagery. a) Overexpanded, Mj = 1.4; b) Perfectly Expanded, Mj = 1.6; c) Underexpanded, Mj = 1.9. From Top to Bottom: Baseline, 24°, and 35° Nozzles.

Select images obtained from the use of schlieren flow visualization are shown in Figure 3-5. The nozzle shown in the images is the 24° beveled nozzle. It can be seen from these images that the jet plume is deflected slightly upwards with increasing M_d. The deflections of the plume for each case were overlaid and are presented in Figure 3-6. Also evident in Figure 3-5 are Mach waves, and appear as lines at 45° from the jet axis. Mach waves are shock waves which occur

from the interaction of supersonic turbulent eddies with the air surrounding the jet plume. As seen in the schlieren images, the Mach wave on the bottom lip is shifted downstream slightly.

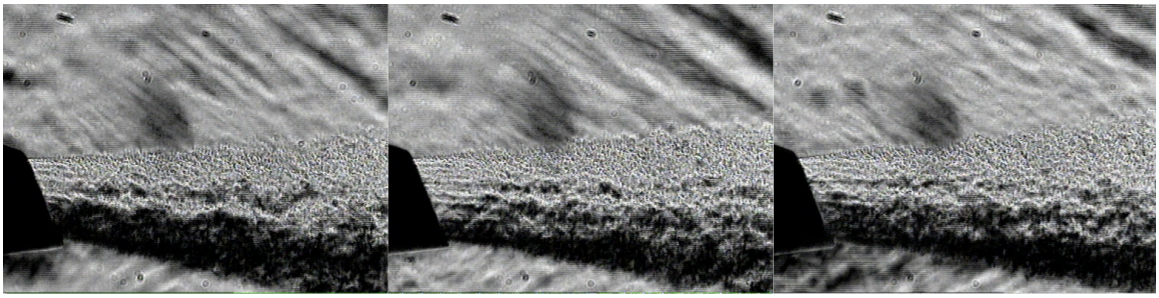

Figure 3-5. Schlieren Imagery of the 24° Bevel at (from left to right) M_d = 1.467, 1.638, 1.771

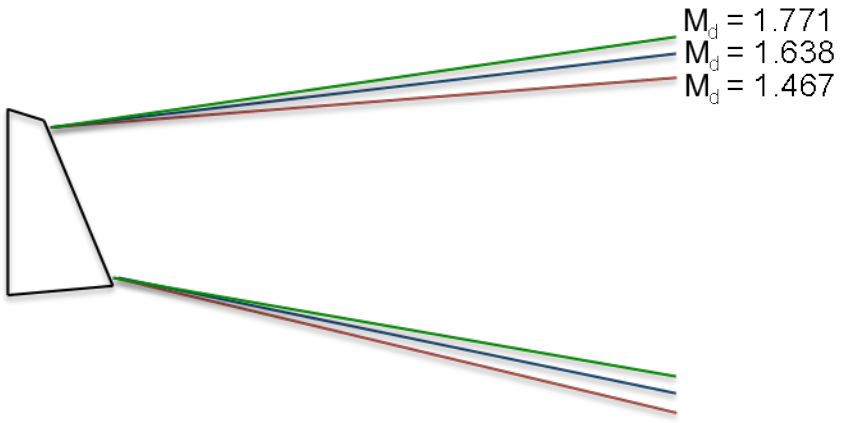

Figure 3-6. Comparison of the Jet Flow for the 24° Bevel at M_d = 1.467, 1.638, 1.771

Acoustic Data

Acoustic experiments were conducted with both cold and heated jets. The density characteristics of heated jet flow were simulated with the use of a mixture of air and Helium. In

this paper acoustic spectra from the heated jets are used because they more closely resemble conditions which would be seen in a military jet during operation. For the acoustic spectra seen in Figure 3-7, Figure 3-8, and Figure 3-9, the total temperature ratio (TTR) is 3 and the characteristic frequency (f_c) is 42693 Hz.

During acoustic measurements the nozzle was oriented in one of two ways, with either the long lip or the short lip facing the microphone array. For each nozzle orientation, acoustic data was taken with the microphone array at two different positions, with the individual microphones covering angles of 20-70° and 80-150°, respectively. Generally acoustic data between the angles of 40° and 50° from the jet axis are of the most interest because the peak emission noise occurs at these angles in military jets. Looking at Figure 3-7, it is apparent that there is a decrease in the noise level when the beveled nozzles are compared to the baseline nozzle at a jet Mach number (M_j) of 1.467. This observation is true when the long lip is oriented towards the microphone array, but in the case where the short lip is facing the microphone array there is no appreciable difference between the baseline and bevel nozzles. For the long-lip case, the noise reduction measured at an angle of 40° from the jet axis is approximately 3.2 dB.

Figure 3-8 shows the acoustic spectra when the jet was run at M_j = 1.638. The spectra shows a smaller reduction in sound levels at 40°, approximately 2.3 dB, when compared to the spectra obtained from the Mj = 1.467 case. This trend continues to the point where, in Figure 3-9 at M_j = 1.771, the noise generated by the baseline nozzle is comparable to each of the beveled nozzles.

It is also of interest to consider the effect that a beveled nozzle has on broadband-shock associated noise (BBSAN) since it is the other major component of high-speed jet noise, aside from the peak emission noise. BBSAN is generated at larger angles than the peak emission noise, generally higher than 100°. For this study we have focused on the noise generated at an angle of

120°. From Figure 3-7, Figure 3-8, and Figure 3-9 it can be seen that the beveled nozzles do not reduce BBSAN at an angle of 120°. For this reason the reduction in the peak emission noise due to the use of beveled nozzles will present the greater consideration in whether beveled nozzles are a successful means of high-speed jet noise reduction.

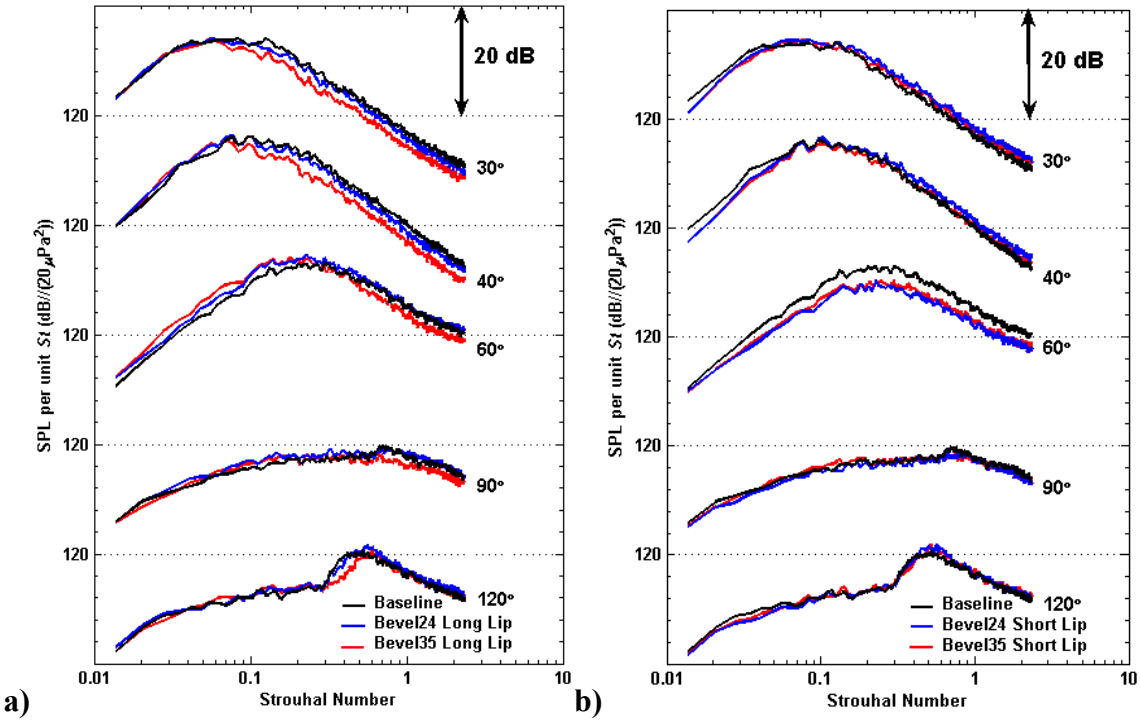

Figure 3-7. Acoustic Spectra, $M_j = 1.467$, $M_d = 1.65$. a) Long Lip Side, b) Short Lip Side.

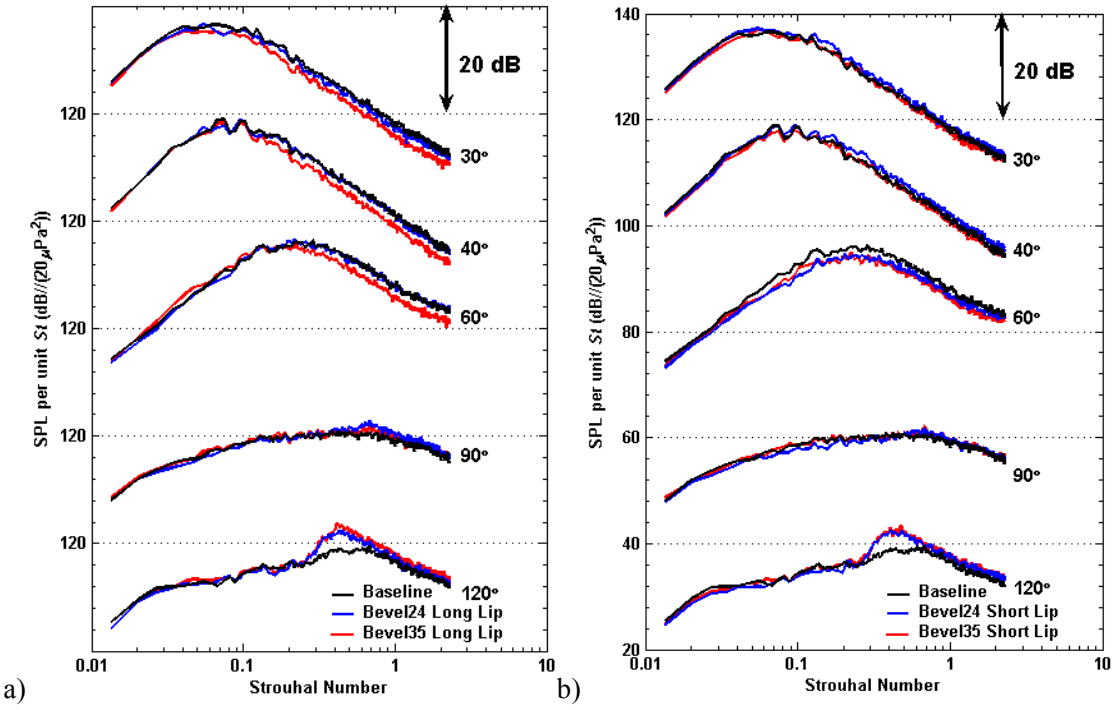

Figure 3-8. Acoustic Spectra, $M_j = 1.638$, $M_d = 1.65$, a) Long Lip Side, b) Short Lip Side.

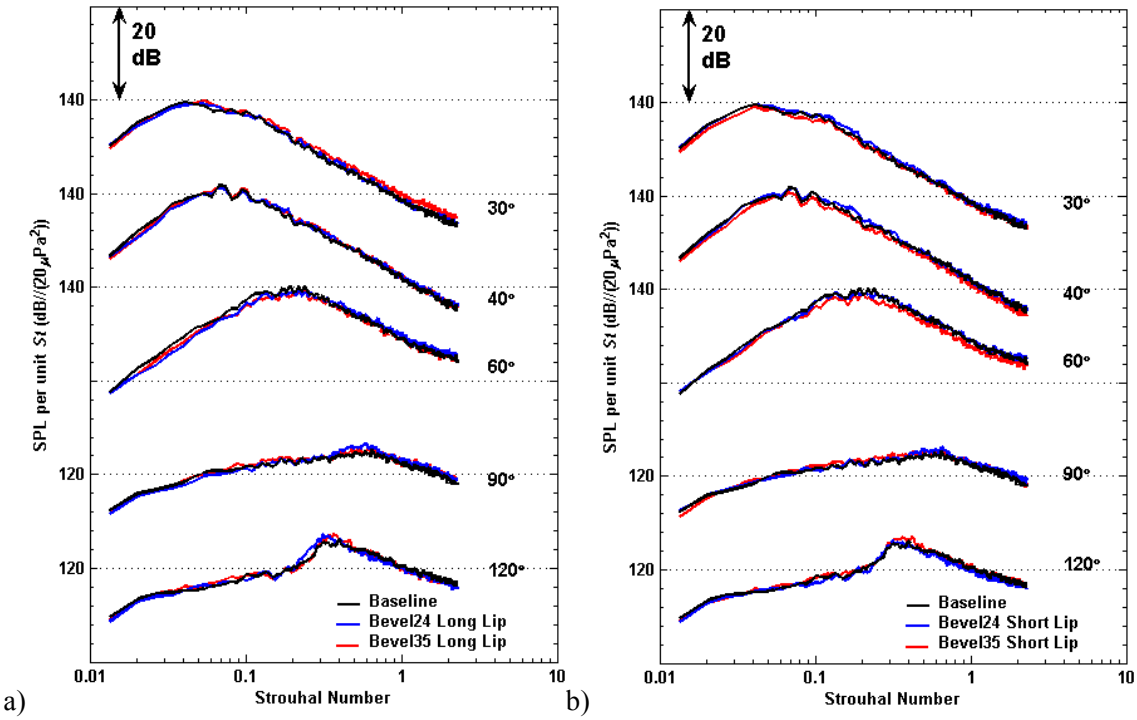

Figure 3-9. Acoustic Spectra, $M_j = 1.771$, $M_d = 1.65$, a) Long Lip Side, b) Short Lip Side.

Chapter 4
Conclusions

This study explored the potential of beveled nozzles as a method of jet noise reduction. After reviewing the acoustic spectra the results are promising, with a decrease of approximately 3.2 dB from the long-lip side during overexpanded conditions in the peak noise emission range. A slightly smaller decrease in noise levels is seen at perfectly expanded conditions, at approximately 2.3 dB. Of these, the noise reduction in overexpanded conditions is the most promising because at take-off military jets operate at over-expanded conditions to maximize their performance. Take-off is one area where a noise reduction would have a huge impact because at that stage of flight the jet is in close proximity to both flight crews and the surrounding community. Additionally, it was found that deflection of the flow was much smaller than that found for purely converging beveled nozzles. The largest deflection of the flow found was 6°.

It is believed that the results obtained from this study using a small-scale heated jet will be very similar for larger scale experiments. Small-scale heated jet experiments have been shown in the past to compare favorably to moderate-scale tests, so it is reasonable to expect that similar tests performed on full-scale platforms will show appreciable reductions in noise levels in the peak noise emission range. However, this is a major area in which future work may be conducted. Another important area which will be explored in greater detail at a later time is noise reduction when the beveled nozzles are oriented to 45°, or sideline noise. Sideline noise is one of the quantities measured when aircraft go through tests to meet noise requirements, so it is also of great interest to reduce noise in this quadrant.

References

[1] Martens, S. and Spyropoulous, J., "Practical Jet Noise Reduction for Tactical Aircraft," *ASME Turbo Expo 2010 Conference*. Glasgow, UK, 2010.
[2] Viswanathan, K., and Czech, M. J., "Adaptation of the Beveled Nozzle for High speed jet Noise Reduction," AIAA Paper No. 2010-654, 2010.
[3] McLaughlin, D. K., Bridges, J., and Kuo, C.-W., "On the scaling of small, heat simulated jet noise measurements to moderate size exhaust jets," International Journal of Aeroacoustics, Vol. 9, No. 4&5, 2010, pp. 627-654.
[4] Kuo, C.-W., Veltin, J., and McLaughlin, D. K., "Acoustic measurements of models of military style supersonic nozzle jets," AIAA Paper No. 2009-18, 2009.
[5] Doty, M. J., McLaughlin, D.K., "Acoustic and mean flow measurements of high-speed, helium-air mixture jets," International Journal of Aeroacoustics, Vol. 2, No. 2, 2003, pp. 293-334.
[6] Settles, G. S., Schlieren and Shadowgraph Techniques, Corrected ed.: Springer, 2001.

VITA

Maureen Senft

Education:

The Pennsylvania State University – The Schreyer Honors College, Aug 2007 – May 2011
Candidate for B.S. in Aerospace Engineering
Expected: May 2011

Work Experience:

Alliant Techsystems (ATK), Spacecraft Systems and Services, May 2010 – August 2010
Technical Intern, Beltsville, MD
-Designed a test fixture which actuates on-orbit satellite servicing tools in functional and thermal tests
-Modeled the test fixture and created technical drawings for manufacturing using Pro/Engineer
-Utilized Geometric Dimensioning and Tolerancing (GD&T) to ensure fit and function of test fixture

Lockheed Martin, IS&GS Civil, June 2009 – August 2009
Senior Technical Intern, Rockville, MD
- Scripted performance and stability tests for Flight Services for the 21st Century
- Designed and implemented a program which discovers areas of performance degradation

Aerospace Engineering Department, Pennsylvania State University, Sept. 2008 – May 2011
Aerospace Research Assistant, University Park, PA
- Studied the effects of beveled jet nozzles on high speed jet noise
- Created a program to interpolate the shape of an airfoil for use in a new wind turbine

Air Force Research Laboratory, Space Vehicles Directorate, May 2008 – August 2008
Phillips Space Scholar: Small Satellite Technician, Kirtland AFB, NM
- Constructed a computer model of the FASTRAC nanosatellite using Solidworks
- Fabricated a model of FASTRAC for a fitcheck and integrated and tested the CUSat nanosatellite
- Collaborated with experts on integration and testing for the TacSat-3 microsatellite